BMC Plant Biology

RESEARCH

Open Access

Integration of transcriptomic and metabolomic analysis reveals light-regulated anthocyanin accumulation in the peel of 'Yinhongli' plum

Bo Xiong[1], Yisong Li[1], Junfei Yao[1], Jialu Wang[1], Linlyu Han[1], Qingqing Ma[1], Taimei Deng[1], Ling Liao[1], Lijun Deng[1], Guochao Sun[1], Mingfei Zhang[1], Xun Wan[1], Siya He[1], Jiaxian He[1] and Zhihui Wang[1*]

Abstract

Background The 'Yinhongli' cultivar of Chinese plum (*Prunus salicina* Lindl.) is characterized by a distinctive bicolored peel phenotype, in which anthocyanins serve as crucial determinants of both its visual characteristics and nutritional quality. However, the molecular mechanism of underlying light-dependent anthocyanin biosynthesis of plum, especially its regulatory network and pathway, need to be further studied and explored.

Results Comprehensive physiological analyses demonstrated distinct pigmentation patterns, revealing that dark-treated (YD) plum peels retained green coloration, whereas light-exposed (YL) and bag-removed samples (YDL) exhibited red pigmentation. Utilizing an integrated approach combining metabolomic and transcriptomic analyses, we identified 266 differentially accumulated flavonoids (DAFs), among which seven anthocyanin metabolites were established as principal determinants of peel coloration. Transcriptomic profiling revealed 6,900 differentially expressed genes (DEGs) between YD and YL, demonstrating significant correlations between the phenylpropanoid and flavonoid biosynthetic pathways. Through Weighted Gene Co-expression Network Analysis (WGCNA) and correlation heatmap analysis, we identified crucial regulatory networks encompassing five structural genes (*PAL*, *4CL*, *F3'H*, *CHI*, and *UFGT*) and 15 candidate regulatory genes, including six light signal transduction factor genes (*UVR8*, *COP1*, *PHYBs*, *PIF3*, and *HY5*) and nine transcription factor genes (*MYB1*, *MYB20*, *MYB73*, *MYB111*, *LHY*, *DRE2B*, *ERF5*, *bHLH35*, and *NAC87*). Subsequent RT-qPCR validation demonstrated significant light-mediated up-regulation of key structural genes (*PAL*, *F3H*, *CHI*, *4CL*, and *UFGT*) involved in anthocyanin biosynthesis along with positive regulatory factors (*DRE2B* and *NAC87*). Conversely, a cohort of negative regulators, including *HY5*, *MYB1*, *MYB20*, *MYB73*, *MYB111*, *LHY*, *ERF5*, and *bHLH35*, showed marked down-regulation in response to light exposure, suggesting their potential repressive roles in the light-dependent anthocyanin biosynthesis pathway.

Conclusions This investigation provides comprehensive insights into the molecular mechanisms of anthocyanin biosynthesis in light-dependent anthocyanin biosynthesis in 'Yinhongli' plum, identifying critical structural genes and

*Correspondence:
Zhihui Wang
wangzhihui318@sicau.edu.cn

Full list of author information is available at the end of the article

potential regulatory TFs. The findings offer substantial contributions to the understanding of anthocyanin regulation in fruit crops and provide a valuable foundation for molecular breeding initiatives aimed at enhancing quality traits in plum cultivars.

Keywords Light, 'Yinhongli' Plum, Anthocyanin biosynthesis, Transcriptomic and metabolomic analysis

Background

The plum plant is extensively cultivated due to its substantial ornamental, nutritional, and medicinal properties [1, 2]. Fruit color is an important indicator for evaluating visual quality and has an important impact on consumer preferences [3, 4]. The primary pigments in plum are anthocyanins, which provide the red and purplish-black coloration [5]. Anthocyanin is an important component of flavonoids, and its biosynthesis encompassing three main stages (phenylpropanoid metabolism, flavonoid metabolism, and anthocyanin synthesis and modification). The process includes structural genes that are involved in enzyme reactions, such as phenylalanine ammonia-lyase (*PAL*), cinnamic acid-4-hydroxylase (*C4H*), 4-coumarate: CoA ligase (*4CL*), chalcone synthase (*CHS*), chalcone isomerase (*CHI*), flavanone 3-hydroxylase (*F3H)*, flavonoid 3'-hydroxylase (*F3'H*), dihydroflavonol-4-reductase (*DFR*), anthocyanidin synthase (*ANS*) and UDP-glucose flavonoid 3-*O*-glucosyltransferase (*UFGT*) [6, 7]. The accumulation of anthocyanin is regulated by the MBW ternary complex [8]. Within this complex, the R2R3-MYB families act as the primary regulator factor, while the bHLH family functions in an auxiliary capacity to either enhance or inhibit the process. Additionally, the WD40 protein plays a supporting role in the complex [9, 10]. Recent research had shown that in the plum cultivar 'Akihime', the R2R3-MYB transcription factor PsMYB10.1, like the peach PpMYB10.1, interacts with PsbHLH3 and PsWD40-1 to enhance gene expression during the stage of anthocyanin synthesis and modification, ultimately promoting anthocyanin biosynthesis [11, 12]. In Japanese plum, there are two *PsMYB10.1* alleles responsible to produce anthocyanin and anthocyanin-less fruit peel color [13]. Other TFs such as bZIP [14], ERF [15], NAC [16], and WRKY [17], primarily influence the accumulation of anthocyanins in fruits of the Rosaceae family by directly or indirectly impacting the *R2R3-MYB* gene groups.

The accumulation of anthocyanins in plants is influenced by the complex interaction of light and plant hormones [18, 19]. In sweet cherry, light stimulated the production of anthocyanin and abscisic acid (ABA), which further enhances the accumulation of anthocyanin [20]. Anthocyanin biosynthesis in various plants, such as *Arabidopsis* [21], apple [22], berry [23], and mango [24], has been found to be induced by light. These investigations have identified phytochromes (PHYs), cryptochromes (CRYs), and UVR8 as the key light receptors integral to this signal transduction pathway. Downstream factors like PIFs, COP1, and HY5 play essential roles in light signal transduction regulation [25, 26]. A significant player in light signal transduction, PyHY5 is known to directly interact with the G-box elements in *PyMYB10* promoter in red pear variety 'Yunhong No.1'. This interaction improves the expression of structural genes (*PyCHS*, *PyANS*, and *PyUFGT*), which ultimately results in a greater accumulation of anthocyanins in the peel [27]. In dark condition, COP1 is capable of regulating HY5 through ubiquitination and subsequent degradation by the 26 S proteasome pathway, establishing its role as an inhibitor [28]. In sweet cherry, COP1 negatively regulates the expression of key structural genes, such as *AtDFR*, *AtLDOX*, and *AtUFGT*, by inhibiting the transcription of *PacMYBA*, thereby resulting in a subsequent reduction in anthocyanin accumulation [29]. Furthermore, the PIFs protein can affect the biosynthesis of anthocyanins in plants by directly or indirectly regulating the *R2R3-MYB* gene families [30, 31].

The influence of light on anthocyanin accumulation in plants can be categorized into light-dependent and light-independent processes [10]. Despite the significance of light-dependent anthocyanin biosynthesis, research on this topic in plum cultivars remains limited. The 'Yinhongli' plum, a Chinese plum (*Prunus salicina* Lindl), serves as an exemplary model for investigating the biosynthesis regulatory mechanism underlying light-induced anthocyanin accumulation due to its striking red peel under direct sunlight and green appearance in partial shade. Here we examined the influence of light on both the aesthetic quality and anthocyanin accumulation in 'Yinhongli' plums. Light treatment induced anthocyanin biosynthesis in the plum peels. Then, we elucidated the associated regulatory networks through transcriptomic and metabolomic analyses. Our investigation identified 15 candidate genes responsive to light in fruit peels and characterized their expression profiles related to the anthocyanin biosynthetic pathway. These findings offer insights into enhancing plum fruit quality as well as understanding the regulatory mechanisms governing light-induced anthocyanin accumulation.

Methods

Plant materials and treatment

Experimental site was in Suining City, Sichuan Province (31°10′N,105°3′E). 450 m above sea level, 17.7 °C average temperature, 1,129 mm of precipitation, and 1,034 h of

sunshine per year are the characteristics of this region [32]. Nine 5-year-old 'Yinhongli' plum plants, cultivated and managed under identical conditions, were chosen as the subjects for the experiment and categorized into three groups, each consisting of three plants. On the 65th days post-anthesis (DPA), about 90 fruits of each 'Yinhongli' plant, located in 5 different directions (east, south, west, north, and center), were bagged for dark treatment (YD). Ten bagged fruits were removed bags (YDL) at 101 DPA from each plum plant. Unbagged fruits were used as light treatment (YL). Double-layered fruit bags with a yellow outer layer and black inner layer (Sichuan Luhai Agricultural Co., Ltd., Sichuan Province, P.R. China) measuring 15 × 18 cm and with a thickness of 0.32 mm were used to prevent fruit exposure to light. The fruitlets were placed in the intermedium stratum of the fruit bags to protect it from damage to the stalk. At least 60 fruits were collected for each sample at 66, 73, 80, 87, 94, 101 and 105 DPA (Mature stage), respectively. After measuring the fruit color, the peels were separated using a scalpel, frozen in liquid nitrogen, and preserved at ultra-low temperature freezer.

Determination of physiological parameters

Throughout the process of plum fruit development, a total of 10 plums for each treatment were chosen at random. As previously described, 3 points on the equatorial line of bagged fruits and in the sunlit area of unbagged fruits were measured using a spectrocolorimeterC164 (X-Rite, MI, USA) [33].

Anthocyanins and flavonoids were extracted using a modified hydrochloric methanol method, based on previous studies [34]. A 1.0 g frozen sample was weighed and mixed with a 5 mL solution of methanol: HCl (99:1, v/v). The mixture was thoroughly oscillated and sonicated for 1 h at 4 ℃. After centrifugation at 8,000 rpm for 15 min at 4 °C, the clear supernatant was collected.

As previously described, we determined the total anthocyanin content in the peel using the pH difference method [35]. Specifically, 1mL of extraction solution was added into 4 mL of pH 1.0 buffer and pH 4.5 buffer, and mixed, respectively. An ultraviolet-visible spectrophotometer (Thermo, MA, USA) was used for measuring the liquid mixture at 513 and 700 nm. Total anthocyanin content levels were expressed as μg/g fresh weight using cyanidin-3-galactoside as standard.

As previously described, we determined the total flavonoid content in the plum peel utilizing the sodium nitrite aluminum nitrate protocol [36]. A solution was prepared by combining 0.1 mL of the extraction solution, 0.9 mL of deionized water, and 0.2 mL of 5% Na_2NO_2. After 5 min, 0.2 mL of 10% Al $(NO_3)_3$ were introduced into the mixture. Subsequently, 2 mL of 4% NaOH and 1.6 mL of deionized water were added after 6 min, followed by allowing the reaction mixture to stand for 15 min at room temperature. The absorbance of the reaction mixture at 510 nm was measured using an ultraviolet-visible spectrophotometer (Thermo, MA, USA). Total flavonoid content levels were expressed as mg/g fresh weight using rutin as standard.

Determination and analysis of flavonoid metabolites

Flavonoid metabolites were determined by Metware Biotechnology Inc. (Wuhan, China), following the method developed by Xiong [37]. In brief, the samples underwent freeze-drying followed by grinding in liquid nitrogen. From these ground samples, 50 mg was extracted by adding 1,200 μL of a 70% aqueous methanol solution. The resulting mixtures were centrifuged at 12,000 rpm for 3 min. Subsequently, the samples were filtered through a 0.22 μm microporous membrane and analyzed for flavonoid metabolites using Ultra Performance Liquid Chromatography (UPLC) coupled with Tandem Mass Spectrometry (MS-MS) (ExionLC™ AD, https://sciex.com.cn/). The UPLC analysis was performed under the following specified conditions: an Agilent SB-C18 column (1.8 μm, 2.1 mm * 100 mm) was utilized; the mobile phases consisted of ultrapure water (containing 0.1% acetic acid) and acetonitrile (also with 0.1% acetic acid). The gradient program initiated with 5% B-phase at 0 min, followed by a linear escalation to 95% B-phase from 0 to 9 min. This 95% proportion was maintained from 9 to 10 min, after which it was reduced back to 5% from 10 to 11 min, remaining at 5% from 11 to 14 min. The flow rate was set at 0.35 mL/min, the column temperature was consistently held at 40 °C, and the injection volume was 2 μL. For mass spectrometry, electrospray ionization was employed, along with specific ion spray voltage conditions. For the analysis of flavonoid metabolites, MWDB (Netware database) and multiple reaction monitoring modes were utilized for qualitative and relative quantification.

Transcriptome analysis

The total RNA from frozen peel samples was isolated using an RNA extraction kit (Tiangen Biotech, Beijing, China). Subsequently, a cDNA library was established and RNA-seq was performed by Metware Biotechnology Inc (Wuhan, China), following the method developed by Li [38]. The resulting RNA sequencing data was submitted to the NCBI's SRA under BioProject ID: PRJNA1061745. Clean data was obtained by filtering adapters and paired reads using the fastp tool. The transcripts were then aligned to the reference genome psalicina_v2.0.fasta.gz, accessible at https://www.rosaceae.org, using the HISAT2 aligner. The FPKM metric was utilized to quantify gene expression levels, while DESeq2 software was employed to identify differentially expressed

genes. The criteria for identification included a fold change of at least 2 and a false discovery rate below 0.05 to ensure robust and significant results in the analysis.

Co-expression network and qRT-PCR analysis

Co-expression Network analysis aimed to identify TFs that regulate genes related to anthocyanin accumulation. The data analysis was carried out via the Metware Cloud online platform. A regulatory network illustrating the co-expression of essential genes associated with anthocyanin accumulation was rendered using Cytoscape version 3.9.1. For RNA isolation and cDNA synthesis, the Plant RNA Extraction Kit (Tiangen Biotech, Beijing, China) and the cDNA Reverse Transcription Kit (Mei5 Biotechnology Co. Ltd, Beijing, China) were employed, respectively. The cDNA served as a template for subsequent analysis, with SYBR Green fluorescent dye being used for the qRT-PCR assessment, which took place on the CFX96 Real-Time PCR Detection System (Hercules, CA, USA). The design of primers for the 16 selected genes (both candidate and structural genes) was performed using Primer Premier5 software, with additional details provided in Table S1. The Actin(enm.TU.Chr6.1716) served as the internal control. The relative gene expression was determined using the $2^{-\Delta\Delta Ct}$ method, adhering to the protocols established by Zhang [39].

Statistical analysis

A one-way ANOVA along with Duncan's test was conducted at the $P < 0.05$ significance level using IBM SPSS Statistics 27.0 software (IBM, New York, USA).

Results

Changes of physiological parameters in Plum fruit after dark treatment

Significant alterations in the peel coloration of 'Yinhongli' plum fruits were observed following YL treatment. Comparative analysis revealed that, in contrast to fruits maintained under dark conditions, the peels of YL exhibited distinct red pigmentation upon light exposure. Furthermore, when fruit bags were removed at 101 days post-anthesis, the peel of YDL similarly demonstrated red coloration under light conditions, indicating a light-dependent pigmentation response (Fig. 1A). During the early stage of YL (66–73 DPA), all fruits were green, and there was no significant difference in the a*/b* (The color

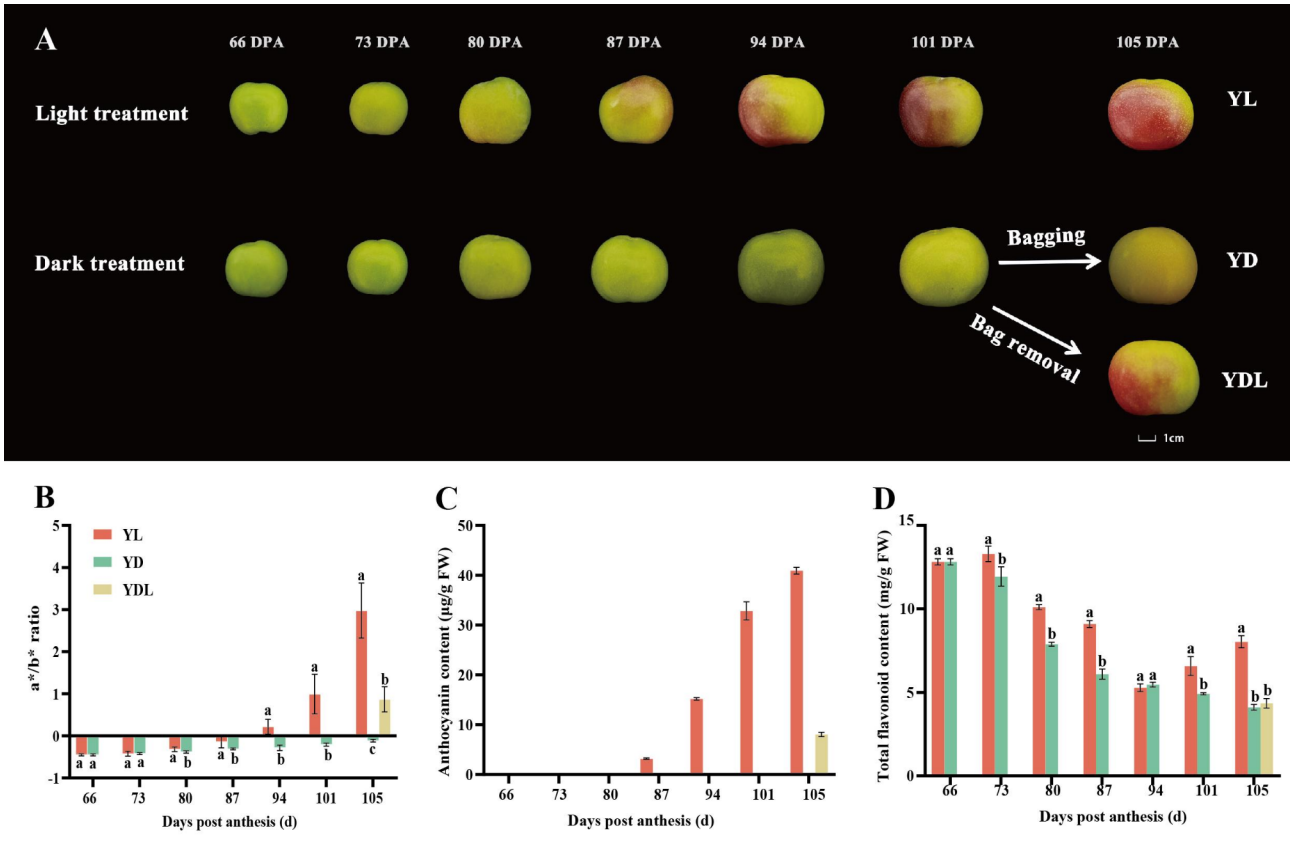

Fig. 1 Effects of dark or light treatments on peel coloration and total flavonoid levels of 'Yinhongli' plums. (**A**) Fruit was initially bagged at 65 days post-anthesis (DPA). At 101 DPA, the bags were removed to expose the 'Yinhongli' plum fruits to light, and samples were collected after four day period. (**B**, **C**, **D**) The a^*/b^* ratio, total anthocyanin content, and total flavonoid content in the peel of 'Yinhongli' plums. Error bars denote the SD derived from three biological replicates. Values in each column bearing distinct letters indicated a significant difference at $P < 0.05$

ratio of comprehensive chromaticity index was calculated according to a and b values) ratio of 'Yinhongli' plum peels. However, at approximately 80 DPA, the a*/b* ratio in certain regions of the YL fruits was significantly higher than that of the YD fruits, which began to turn white. Subsequently, both the YL and YDL exhibited an increase in the a*/b* ratio as their peel color shifted to red, while the YD remained negative (Fig. 1B). The changes in fruit peel color were consistent with the total anthocyanin content observed in YL and YDL, whereas no anthocyanin was detected in the peel of YD (Fig. 1C). The trend of total flavonoid content accumulation in the peels of 'Yinhongli' plums showed clear variations after the YD. The flavonoid content in the peel of YL initially decreased and then increased, while for the YD, the content continued to decline throughout development. The total flavonoid content in the peel of YL decreased to its lowest level of 5.28 mg/g, which did not significantly differ from that of the YD (Fig. 1D). Based on above physiological parameter change profiles, samples from the two treatments at 87, 94, and 105 DPA were selected for metabolome and transcriptome analysis.

Analysis of flavonoid metabolome

A total of 402 flavonoids have been identified in the peels of YL and YD, which could be classified into ten classes: 21 chalcones, 35 flavanones, 12 flavanonols, 91 flavones, 164 flavonols, 36 flavanols, 11 isoflavones, 8 anthocyanins, 13 proanthocyanidins, and 11 other flavonoids. Among the ten classes of flavonoids identified, it was found that the highest proportion was observed in the case of flavonols (40.8%), while the lowest proportion was seen for anthocyanins (2%) (Fig. 2A, Table S2). Furthermore, analysis of principal components (PCA), performed to analyze the differences in data among the samples, showed a high correlation between replicates. The reliability of the data was also confirmed by Pearson's correlation coefficient. It was revealed through PCA that PC1 (33.83%) and PC2 (17.95%) together explained about 51.78% of the differences between samples indicating that there was a dynamic change pattern during 'Yinhongli' plum peel development. The specific accumulation of certain types of flavonoids observed can be attributed to their differential responses to light treatments as indicated by PC1 (Fig. 2B).

By setting the threshold for variable importance in projection (VIP) to greater than considering a fold change difference of either ≥2 or ≤0.5, we identified a total of 266 DAFs. When comparing the YD and YL samples at different stages, it was observed that the group with the highest number of DAFs was YD105 vs. YL105 (a total of 173 DAFs, with 151down-regulated and 22 up-regulated),

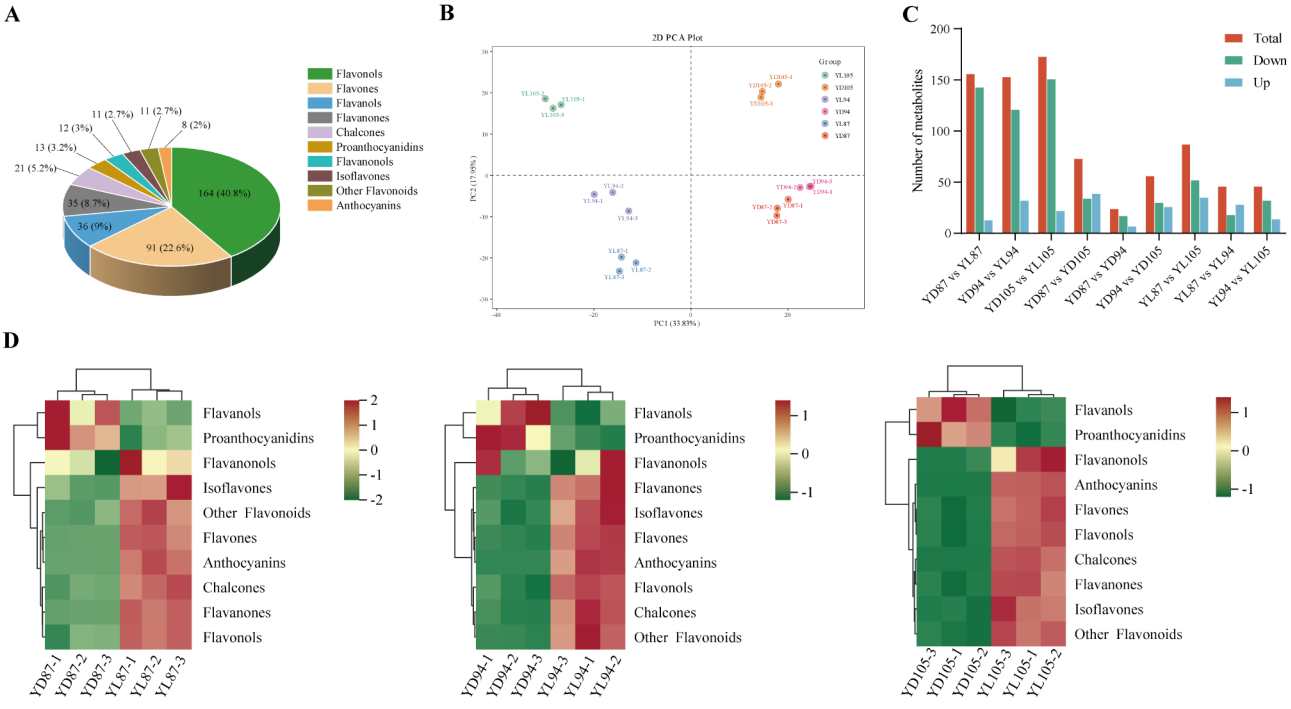

Fig. 2 Analysis of metabolomic data for peel at three different stages following dark (YD) and light (YL) treatments. (**A**) The composition and distribution of 402 flavonoids in YL and YD peel samples were examined. (**B**) Principal component analysis (PCA) was performed to assess the metabolites in two treatment groups at three time points. (**C**) The number of DAFs was determined for the overall (red), upper (green), and lower (blue) color tones across the four time periods. (**D**) A heatmap was generated to illustrate the abundance of 10 classes of flavonoids in YL and YD peels over the three developmental stages. Regions in red indicate a high content, while those in green signify a lower content

while the groups with the fewest DAFs were YL87 vs. YL94 and YL94 vs. YL105. In general, there was a higher number of DAFs that were down-regulated throughout the three stages. This consistency was in line with the observed variation in total flavonoid content, ultimately confirming the precision of physiological parameter assessment (Fig. 2C, Table S3).

General heatmap revealed that YL peels had higher total flavonoid content compared to YD peels, with flavanonols, flavanones, isoflavones, flavones, anthocyanins, flavonols, chalcones, and other flavonoids contributing to this difference. Conversely, only flavanols and proanthocyanidins made significant contributions to the total flavonoid content in the YD peels (Fig. 2D). The content of 7 anthocyanin components (include 4 cyanidins, 1 delphinidin, and 2 peonidins) in the peel of YL saw a significant up-regulation indicating a direct relationship between anthocyanin accumulation and red color formation (Fig. 3A-G). The findings suggested that dark and light treatments may alter the original pattern of flavonoid biosynthesis in the peel.

Transcriptome analysis

After high-throughput sequencing, we obtained 40,152,180 to 47,000,500 clear reads, resulting in a total of 118.64Gb clean base with Q20 and Q30 statistics exceeding 98.07% and 94.3%, respectively. When mapped to the reference genome of the 'Sanyueli' plum, the alignment rate was higher than 94.30%, among them more than 87.39% were uniquely mapped (Table S4). 26,880 expression genes were obtained through transcript assembly and removal of non-expressed genes. These

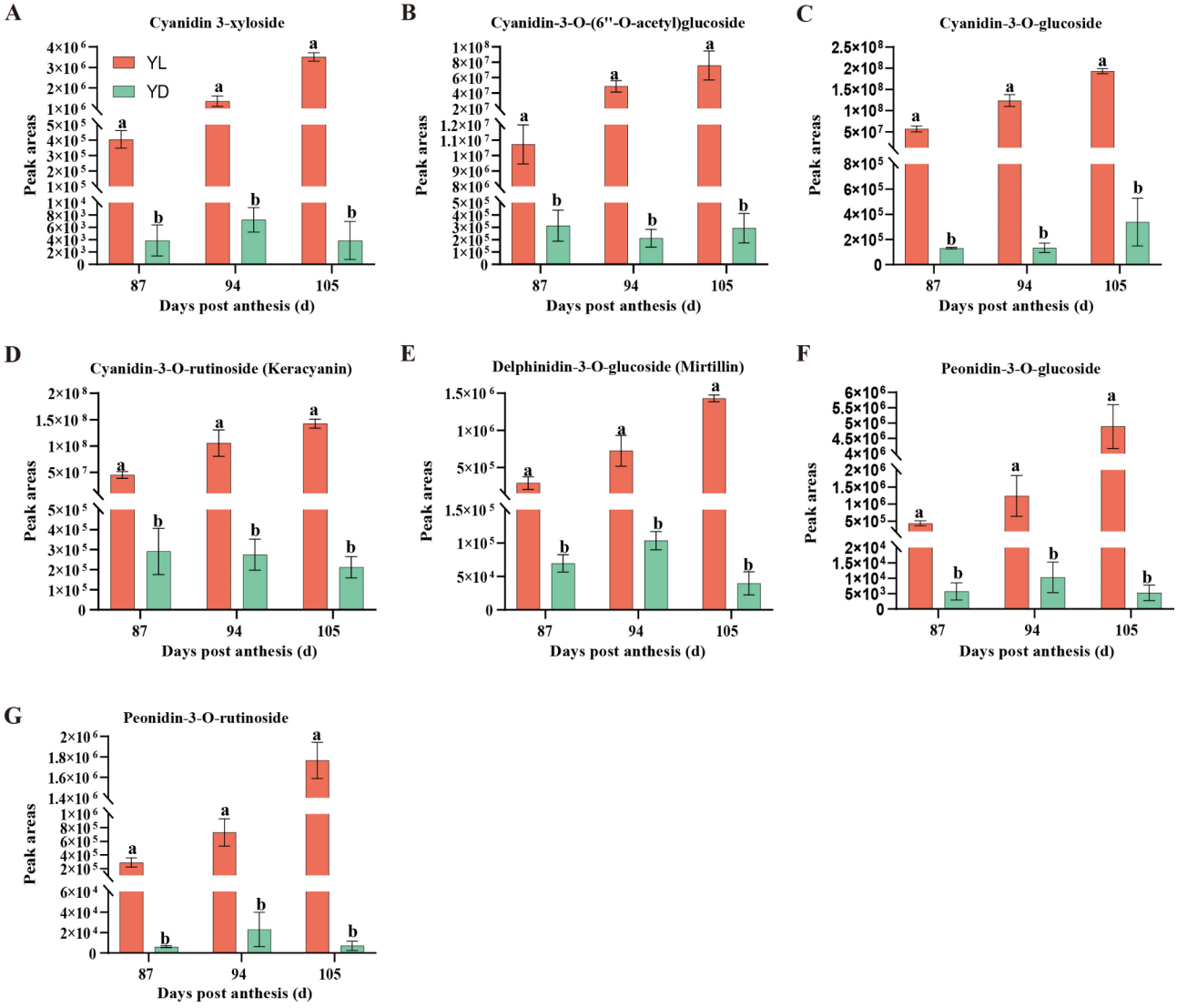

Fig. 3 Peak areas of 7 different anthocyanin components identified in three different stages following two treatments. Significance was evaluated using t-test. Different letters in each column indicate significant differences ($P < 0.05$)

genes were then annotated using public databases such as GO, KEGG, KOG, NR, Swiss-Prot, Tremble, and Plant-TFDB (Table S5).

PCA was used to analyze the transcript expression of the samples. YL and YD samples exhibited a distinct separation on the score plot, indicating that light or dark treatment influenced the transcripts of the peel. In contrast to flavonoids accumulation, the proximity between YL94 and YL105 suggested similarity in gene expression during the late stage of fruit ripening (Fig. 4A). 6,900 DEGs were identified through differential expression analysis comparing two treatments (light and dark) and three treatment times (87, 94, and 105 DPA). Based on the quantitative analysis of DEGs, the difference between treatments was slightly smaller than that between treatment times (Fig. 4B, Table S6).

Based on the annotation of the GO database, the top 50 significantly enriched GO terms were classified into several classifications: molecular function (MF), cellular component (CC), and biological process (BP). The majority of DEGs were divided into BP and MF, including phenylpropanoid metabolic process, phenylpropanoid biosynthetic process, glucosyltransferase activity, photosynthesis, flavonoid biosynthetic process, photosynthetic electron transport chain, and light reaction ($P < 0.001$, Fig. 4C). Subsequently, KEGG enrichment analysis was conducted to explore the metabolic pathways in which these DEGs were involved during peel coloring. These DEGs were mainly associated with flavonoid biosynthesis (51 genes), plant hormone signal transduction (232 genes), phenylpropanoid biosynthesis (91 genes), photosynthesis (39 genes), glycolysis/gluconeogenesis

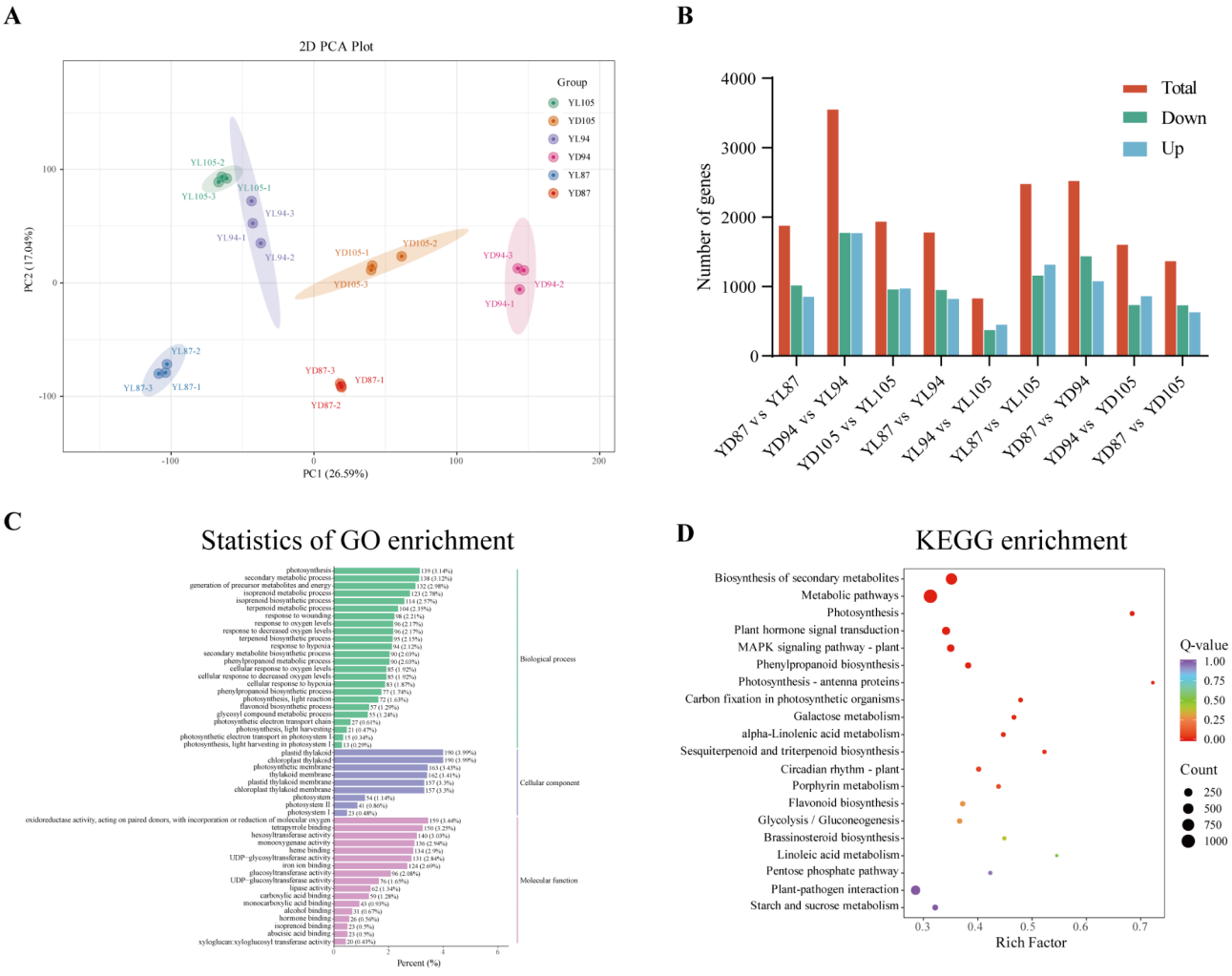

Fig. 4 Analysis of transcriptome data for peel at three different stages following dark (YD) and light (YL) treatments. (**A**) Principal component analysis (PCA) of gene expression in two treatment groups during three stages. (**B**) Statistical analysis of the number of DEGs across three stages, where green indicates down-regulated, blue indicates up-regulated, and red represents the total quantity of DEGs. (**C**) Column charts showing GO enrichment for DEGs in YL and YD, respectively. (**D**) Circular diagram depicting KEGG enrichment for DEGs in YL and YD, respectively. Bubble sizes denote the DEG count, while bubble color corresponds to Q-values

(55 genes), starch and sucrose metabolism (74 genes) (Fig. 4D).

Alteration of the anthocyanin biosynthesis pathway in pigmentation of Peel

According to the annotation of public databases and flavonoid pathways in some model plants, 33 anthocyanin biosynthesis structural genes were identified. Heatmap analysis revealed that one *PAL* (evm.TU.Chr6.2407), one *4CL* (evm.TU.Chr2.3181), one *CHS* (evm.TU.Chr1.5839), one *CHI* (evm.TU.Chr2.2618), two *F3'Hs* (evm.TU.Chr5.440, novel.3206), and two *UFGTs* (evm.TU.Chr7.1822, evm.TU.Chr2.3164) were highly expressed in YL peels, with their expression levels progressively increased over time and peaking at 105 DPA. Conversely, one *F3H* (evm.TU.Chr5.1962), one *DFR* (evm.TU.Chr8.1929), one *ANS* (evm.TU.Chr3.1923), and two *UFGTs* (evm.TU.Chr1.5084 and evm.TU.Chr1.5086) exhibited higher expression levels in YL peels that decreased with prolonged light exposure. Additionally, one *PAL* (evm.TU.Chr2.2113), five *4CLs* (evm.TU.Chr1.2268, evm.TU.Chr1.3516, evm.TU.Chr1.5110, evm.TU.Chr6.1049, and evm.TU.Chr3.1099), four *CHIs* (evm.TU.Chr1.1816, evm.TU.Chr1.1817, evm.TU.Chr2.2237, and evm.TU.Chr8.2485), four *F3Hs* (evm.TU.Chr1.1675, evm.TU.Chr1.846, evm.TU.Chr2.2487, and evm.TU.Chr7.2860), and one *DFR* (evm.TU.Chr1.2057) exhibited elevated expression levels specifically in YD peels(Fig. 5A). Subsequently, to clarify the relationships between the seven differentially accumulated anthocyanin metabolites and 33 structural genes involved in anthocyanin biosynthesis, a correlation heatmap analysis was conducted. The results revealed that *PAL* (evm.TU.Chr6.2407), *UFGT* (evm.TU.Chr2.3164), *F3'H* (novel.3206), and *CHI* (evm.TU.Chr2.2618) exhibited highly positive correlations with seven differentially accumulated anthocyanin metabolites ($r \geq 0.9$, $p \leq 0.001$), while *4CL* (evm.TU.Chr6.1049) showed strong negative correlations with these metabolites ($r \leq 0.9$, $p \leq 0.001$). These findings suggest that these five structural genes might be involved in the regulation of anthocyanin accumulation (Fig. 5B).

WGCNA of DEGs and anthocyanin biosynthesis genes

To further elucidate the biosynthesis regulation mechanism underlying light-induced anthocyanin accumulation resulting in a color change in the peel, we subjected a total of 6,900 DEGs to WGCNA. To create a co-expression network, a threshold of 20 was chosen, resulting in the construction of a gene dendrogram that visually represented the unique clusters of interconnected genes (Fig. 6A). A total of 6,900 DEGs were categorized into 11 distinct modules. Among these, the grey module had the lowest number of DEGs, totaling 57, while the turquoise module comprised the highest number, with 2,470 DEGs (Fig. 6B). Subsequently, we used the gene expression levels of 5 crucial structural genes as trait indicators and conducted correlation analysis with the 11 modules (Fig. 6C). The turquoise module demonstrated a positive correlation solely with *4CL* (evm.TU.Chr6.1049) ($r = 0.87$, $p < 0.001$). In contrast, the yellow module exhibited positive correlations with the gene expression levels of *PAL* (evm.TU.Chr6.2407) ($r = 0.95$, $p < 0.001$), *F3'H* (novel.3206) ($r = 0.91$, $p < 0.001$) and *UFGT* (evm.TU.Chr2.3164) ($r = 0.91$, $p < 0.001$). Visualization of the gene expression patterns within the modules was achieved through column charts and heatmaps. The continuous increase in the gene expression level of YL within the yellow module was notably higher than that of YD. Above finding was in line with the evolving trend of 7 anthocyanin components and total anthocyanin content (Fig. S1). Analysis of KEGG enrichment showed that the yellow and turquoise modules' genes were enriched in metabolic pathways associated with anthocyanin production, such as flavone and flavonol biosynthesis, flavonoid biosynthesis, and phenylpropanoid biosynthesis (Fig. S2). Therefore, we identified the yellow and turquoise modules as the key modules for studying crucial genes. Taking advantage of the strong positive correlation between gene expression levels and structural genes, a gene co-expression network was constructed. The network diagram identified six light signal transduction factors (*UVR8*, *COP1*, *PHYBs*, *PIF3* and *HY5*) involved in the photomorphogenesis. In the interaction network diagram, 9 transcription factors (TFs) in the outer layer were found to be strongly correlated with 5 structural genes. These TF genes included 5 *MYBs* (*MYB1*, *MYB20*, *MYB73*, *MYB111* and *LHY*), 2 *ERFs* (*DRE2B* and *ERF5*), 1 *bHLH* (*bHLH35*) and 1 *NAC* (*NAC87*). Therefore, the study identified 6 light signal transduction factors and 9 TFs as candidate genes for light-induced anthocyanin accumulation in 'Yinhongli' plum peel (Fig. 6D).

Validation of the accuracy of transcriptome data

To verify the transcriptome data's accuracy, we chosen specific genes from both candidate and structural gene pools of the DEGs for qRT-PCR validation (Fig. 7). The selected genes exhibited varying responses to the two treatments across different time points. Light treatment significantly induced the expression levels of *PAL*, *F3'H*, *CHI*, *4CL*, and *UFGT* genes in 'Yinhongli' plum. Compared with dark treatment, the expression levels of the above structural genes showed a continuous upward trend under light conditions, and their dynamic changes were significantly correlated with the anthocyanin accumulation process. We speculated that these genes may be involved in the anthocyanin biosynthesis pathway as key structural genes. It is worth noting that the expression

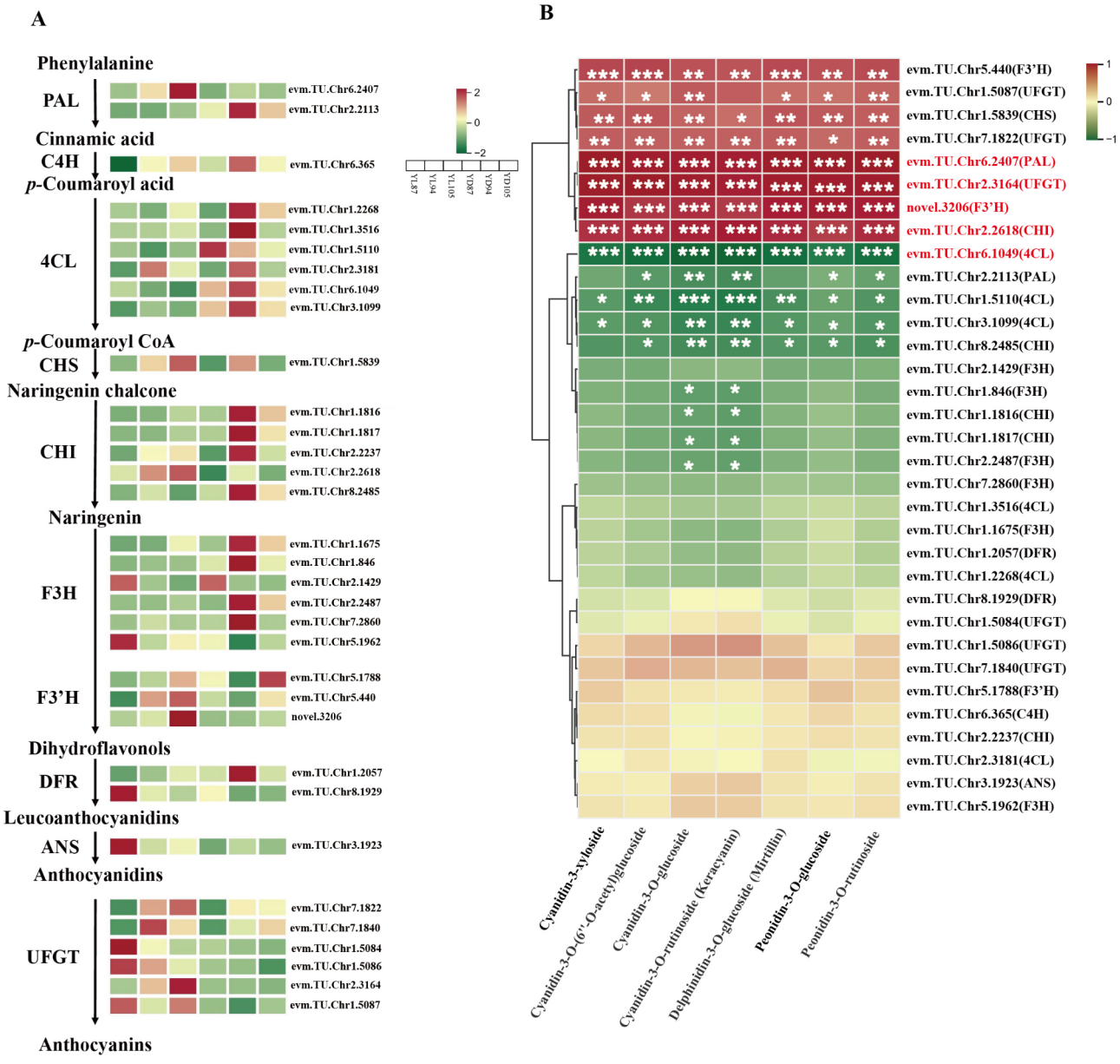

Fig. 5 Assessment of components DEGs in the biosynthesis of anthocyanins. (**A**) Detection and description of expression patterns for structural genes. The rows in the heatmaps correspond to gene identification and the columns represent the samples. The heatmap cell colors reflect the normalized FPKM values of gene expression as well as the relative content of anthocyanin compounds. (**B**) Pearson's correlation analysis between anthocyanin biosynthesis structural gene expression levels and differential accumulation anthocyanin components relative content. Regions in red indicate a positive correlation, while those in green signify a negative correlation. The red text represents 5 critical structural genes. Significance levels denoted by: *, $P < 0.05$, **, $P < 0.01$, and ***, $P < 0.001$ as determined by t-test

patterns of *DRE2B* and *NAC87* transcription factors were highly similar to those of structural genes, indicating that they may be potential positive regulators in anthocyanin biosynthesis. Furthermore, the low expression of *HY5*, *MYB1*, *MYB20*, *MYB73*, *MYB111*, *LHY*, *ERF5*, and *bHLH35* under light treatment indicates that they may be potential negative regulators in anthocyanin synthesis. The qRT-PCR verification experiment further confirmed that the expression patterns of anthocyanin biosynthesis-related structural genes and their regulatory factors were different under the two treatment conditions. The results showed that the biosynthesis of anthocyanin in 'Yinhongli' plum was related to the above structural genes and transcription factors.

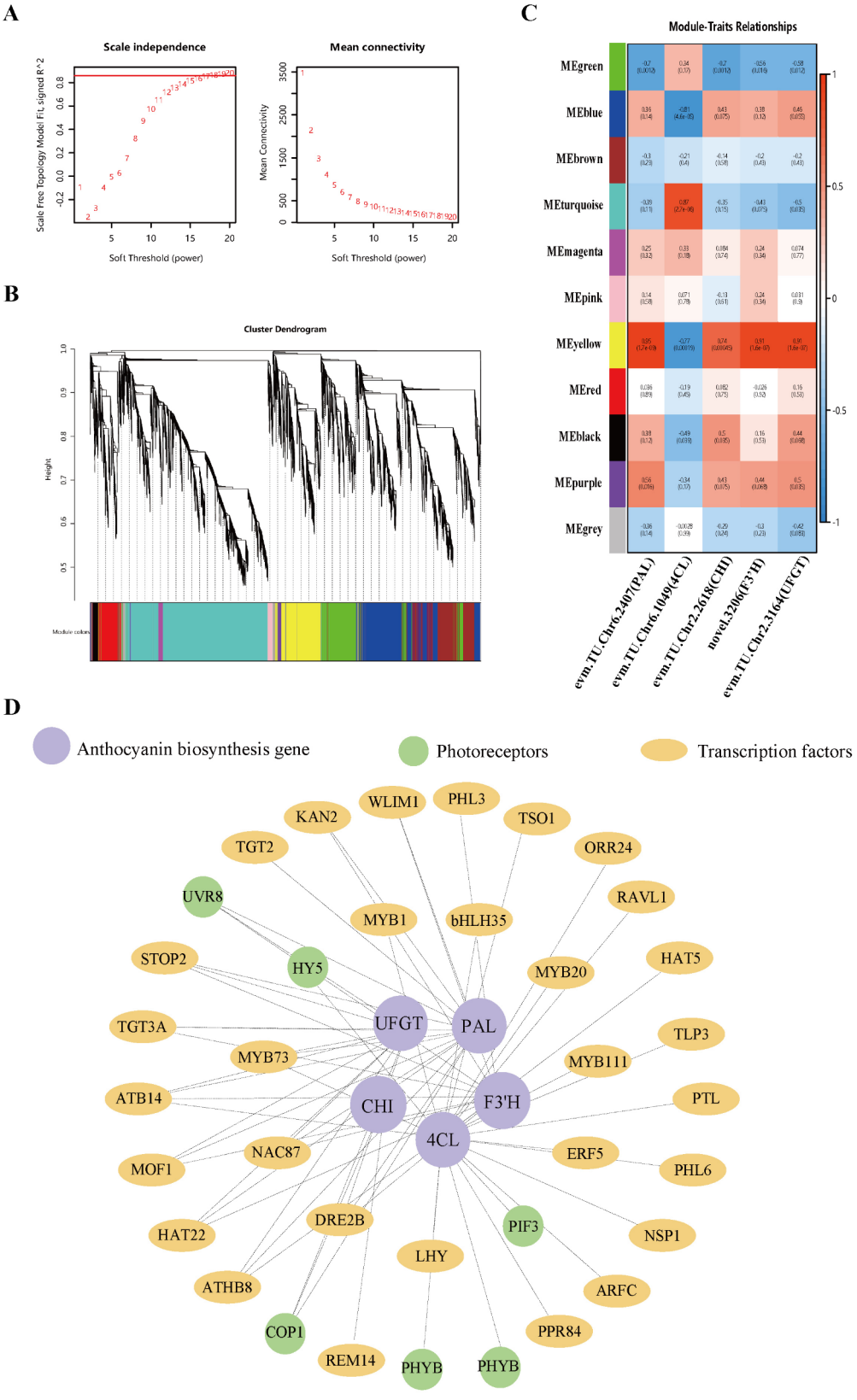

Fig. 6 (See legend on next page.)

(See figure on previous page.)

Fig. 6 WGCNA of DEGs and anthocyanin biosynthesis genes in YL and YD. (**A**) The calculation of the soft threshold was conducted as follows. The x-axis displays the soft threshold (β), while the y-axis represents the scale-free network model index. The average link degree for each soft threshold is shown in the plot. (**B**) Heatmap plot of the gene network depicting co-expression modules. (**C**) Heatmap showing the relationship between modules and traits. Regions in red indicate a positive correlation, while those in blue signify a negative correlation. (**D**) Interaction network diagram displaying DEGs in the yellow and turquoise modules. Green and yellow nodes denote light signal transduction factors and transcription factors, respectively. These nodes have been annotated and identified using public databases

Discussion

Anthocyanins, a group of compounds responsible for the red color in flavonoids, are crucial in determining the visual quality and economic value of the 'Yinhongli' plum [33]. Light is a key factor in the accumulation of anthocyanins [20]. The red peel was only observed on unbagged and bag-removed fruits, whereas bagged fruits had a contrasting appearance, suggesting that the development of bi-colored fruits was influenced by light. The rapid reddening of the bag removal fruit may be caused by the increased sensitivity to re-exposure to light [40], consistent with similar research on other fruits [23, 24, 41]. In addition, light also affected the accumulation of other flavonoids [42]. Compared with dark treatment, buckwheat sprouts under light can accumulate more flavonoids [43]. Solar ultraviolet radiation significantly enhanced the accumulation of anthocyanins and flavonols in apples, while exhibiting minimal impact on proanthocyanidins biosynthesis [44]. Increasing far-red and near-infrared light can lead to a buildup of flavonoid methyl derivatives in tobacco plants while simultaneously hindering the production of flavonoid glycoside derivatives [45]. In this study, we observed that the total flavonoid content decreased during bagging, while the level of flavanols and proanthocyanidins increased significantly. Consequently, our findings indicated that dark treatment modified the original biosynthesis patterns during fruit ripening.

Transcriptome sequencing provides an important reference for examining the expression profiles of plant genomes during various developmental stages and environmental factors [46]. Recently, the transcriptome analyses on berries [23], mango [24], apples [41], and kiwifruit [47] have been conducted under dark treatment, all revealing that transcriptional reprogramming occurs in response to dark treatment, consistent with findings from 'Yinhongli' plum peels (Fig. 4A). Analysis of enrichment revealed that most of DEGs were associated with photosynthesis and flavonoid biosynthesis (Fig. 4C, D). Previous studies have demonstrated that certain signals dependent on chloroplast function also play an important role in biosynthesis of flavonoid compounds. For example, sucrose produced by photosynthesis in *Arabidopsis* can activate anthocyanin biosynthesis, while knocking out triose-phosphate/phosphate translocator or using 3-(3,4-dichlorophenyl)-1,1-dimethyl urea to block photosynthetic electron transport chains can inhibit flavonoid biosynthesis [48–50]. As a result, we hypothesized that light exposure is crucial for the synthesis of anthocyanins in the peels of 'Yinhongli' plums.

New research indicates that the alteration in color change of red-skinned fruits is linked to the quantity of structural genes expressed in the process of generating anthocyanins [11, 33]. Light exposure has been shown to stimulate the expression of key genes *MdCHS*, *MdANS*, and *MdUFGT*, leading to the production of anthocyanin in apple (*Malus domestica*) [51]. Our analysis of gene expression revealed that light activates genes associated with anthocyanin biosynthesis and modification processes in the peel, potentially explaining the influence of light on peel color (Fig. 5A). Furthermore, through the WGCNA analysis, we identified two modules (yellow and turquoise) that were linked to anthocyanin biosynthesis structural genes (Fig. 6C). Additionally, we identified 15 potential candidate genes that may affect anthocyanin production by directly interacting with specific structural gene promoters, thereby regulating anthocyanin accumulation in response to light exposure (Fig. 6D). We selected specific genes from both candidate and structural gene pools of the DEGs for qRT-PCR validation. RT-qPCR results showed that *PAL*, *F3'H*, *CHI*, *4CL*, and *UFGT* were highly expressed under light treatment, the expression pattern of *DRE2B* and *NAC87* is similar to that of the 5 structural genes, indicating that they might be key structural genes and potential positive regulators in anthocyanin biosynthesis. Furthermore, the low expression of *HY5*, *MYB1*, *MYB20*, *MYB73*, *MYB111*, *LHY*, *ERF5*, and *bHLH35* under light treatment indicates that they may be potential negative regulators in anthocyanin synthesis (Fig. 7).

The R2R3-MYB transcription factor family members achieve different functions in the transcriptional regulation of anthocyanins through the C-terminal transcriptional activation and inhibition domains [52]. In *Arabidopsis*, *R2R3-MYB* members *AtMYB75*, *AtMYB90*, and *AtMYB111* encode transcription factors that act as activators by interacting with bHLH members to increase anthocyanin accumulation, while those from *AtMYB4*, *AtMYB7*, and *AtMYBL2* reduce anthocyanin and other flavonoids production by repressing the expression of *AtDFR* and *AtTT8* to maintain pigment balance [53, 54]. Furthermore, both *AtMYB75* in Arabidopsis and *MdMYB1* in apple are positive regulators of anthocyanin production that are stimulated by light [55, 56]. The strawberry *FaMYB1* has a motif like to that of *AtMYB4*

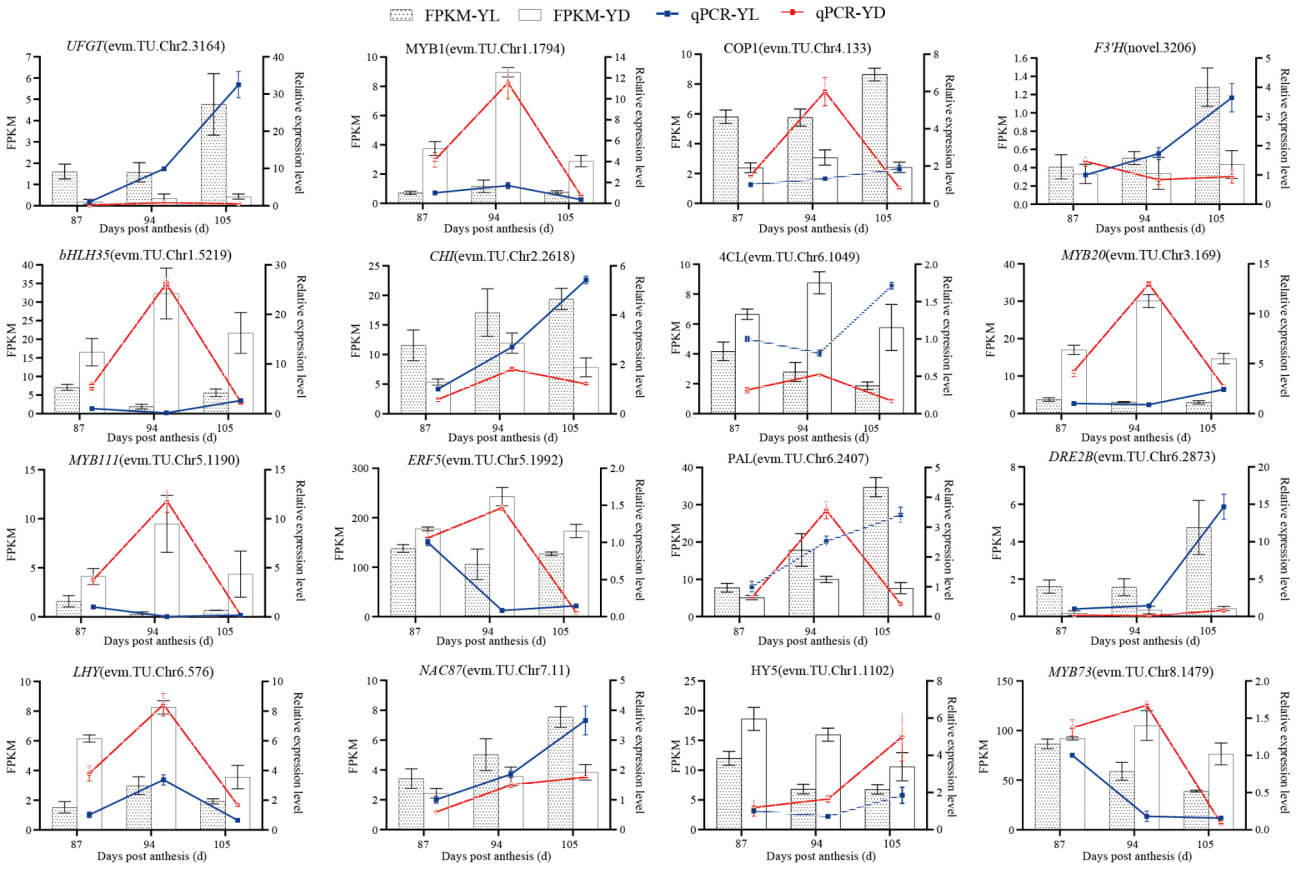

Fig. 7 Analysis of expression levels for genes involved in light-induced anthocyanin accumulation in the 'Yinhongli' plum peel under dark (YD) and light (YL) treatments. Actin served as the internal control. Error bars denote the SD derived from three biological replicates. The left y-axis displays the RNA-seq expression data. The right y-axis illustrates relative gene expression levels assessed by qRT-PCR

at the C-terminus. FaMYB1 and AtMYB4 genes encode transcription factors that form complexes with the transcription factor encoded by FabHLH3 resulting in inhibition of flavonoid biosynthesis structural gene expression which consequently reduces the biosynthesis of cyanidin 3-rutinoside and quercetin-glycosides [57]. *PsMYB10*, a member of R2R3-MYB family in plums, is recognized as a crucial gene in the regulation process of anthocyanin biosynthesis in the peel [13]. In 'Wushancuili', it was speculated that the lack of anthocyanin was due to the loss of function of the *PsMYB10* sequence [58]. The interaction between PsMYB10.1 and PsMYB10.2 with PsbHLH3 activates the expression of anthocyanin biosynthesis structural genes, resulting in the increase of anthocyanin content [11, 59]. Furthermore, the interaction between PsERF1B and PsMYB10.1 enhanced the expression level of *PsUFGT* and increased total anthocyanin content [15]. In the peel of 'Yinhongli' plum, we discovered five MYB families that are closely associated with the structural genes (Fig. 6D, Table S8). The *Arabidopsis* homologs were *AtMYB1* and *AtMYB111*, which are activated by light and regulate the expression of structural genes [56, 60]. By comparison, the response of the identified differentially expressed *MYBs* to light was opposite to that of *Arabidopsis* homologs, suggesting that their roles in the 'Yinhongli' plum may be at least partially different from their functions in *Arabidopsis*.

In plants, HY5, PIF, and COP1 are essential components of light signal transduction and are crucial in photomorphogenesis [61]. HY5 not only directly binds to the promoters of anthocyanin biosynthesis structural genes *CHS*, *F3H*, and *UFGT* to regulate anthocyanin accumulation, but also interacts with the promoter of R2R3-MYB transcription factor family members or other TFs to activate the R2R3-MYB family, thereby facilitating anthocyanin biosynthesis [23]. The bZIP transcription factor HY5 positively regulated biosynthesis of anthocyanins by binding to the promoter of *MdMYB10* and up-regulating the expression level of *MdNAC52*, which in turn promotes anthocyanin accumulation by regulating the transcription of *MdMYB9* and *MdMYB11* in apple [62, 63]. In the model plant *Arabidopsis*, the regulatory effect of PIFs in the regulation of anthocyanin biosynthesis were intricated. While AtPIF3 interacts with AtHY5 to activate the transcription of structural genes and enhance anthocyanin accumulation, AtPIF4 inhibits

anthocyanin biosynthesis by competing with AtTT8 for the binding site of AtMYB75 [31, 64]. Light receptor proteins respond to different light wavelengths by interacting with positive transcription factors or inhibiting COP1, ultimately regulating downstream gene transcription [65]. In the eggplant cultivar 'Lanshanhexian', light exposure primarily triggers anthocyanin accumulation in the peel. This process involves up-regulation of SmCRY1 and SmHY5 expression, along with down-regulation of SmCOP1. SmCRY1 interacts with SmCOP1 to deactivate it, allowing SmHY5 to bind to the promoters of *SmMYB1*, *SmCHS*, and *SmDFR*, thereby enhancing their expression levels and promoting anthocyanin accumulation [66]. Here we found that photoreceptors in the 'Yinhongli' plum peel exhibited distinct responses to light. Specifically, UVR8 and COP1 displayed opposite gene expression patterns under light (Table S8). Previous research has found that the monomer generated by UVR8 protein cleavage under UV-B light may potentially interact with COP1 to form UVR8-COP1-SPA complex, consequently promoting the stability of HY5 and creating a favorable environment for anthocyanin accumulation [10]. Co-expression network analysis further revealed that these genes may ultimately target anthocyanin biosynthesis genes. Therefore, we hypothesized that light regulated the accumulation of anthocyanin in the peel through the HY5-dependent pathway.

Conclusion

In conclusion, metabolomics analysis revealed that light exposure was essential for anthocyanin biosynthesis in 'Yinhongli' plum, with dark treatment completely inhibiting pigment accumulation and seven anthocyanin metabolites were established as principal determinants of peel coloration. Transcriptomic analysis demonstrated significant correlations between the phenylpropanoid and flavonoid biosynthetic pathways. WGCNA and qRT-PCR analysis suggested that structural genes (*PAL*, *4CL*, *F3'H*, *CHI*, and *UFGT*) that might be involved in the light-regulated anthocyanin synthesis of 'Yinhongli' plum. The TF genes *DRE2B* and *NAC87* were highly expressed under light, suggesting that they might be potential positive regulators of anthocyanin biosynthesis. Light signal transduction factors *UVR8*, *COP1*, *PHYBs*, *PIF3* and *HY5* and TF genes *MYB1*, *MYB20*, *MYB73*, *MYB111*, *LHY*, *ERF5*, and *bHLH35* were lowly expressed in YL, suggesting that they might have played negative regulatory role in anthocyanin biosynthesis. However, the specific regulatory mechanism between these transcription factors and structural genes warrant further investigation.

Abbreviations

DAFs	Differentially accumulated flavonoids
DEGs	Differentially expressed genes
WGCNA	Weighted Gene Co-expression Network Analysis
YD	Dark treatment
YDL	Bagged fruits were removed bags
YL	Light treatment
DPA	Days post-anthesis
PCA	Analysis of principal component
VIP	Variable importance in projection
TFs	Transcription factors

Supplementary Information

The online version contains supplementary material available at https://doi.org/10.1186/s12870-025-06414-z.

Supplementary Material 1

Supplementary Material 2

Acknowledgements

Not applicable.

Author contributions

Bo Xiong: Data curation, Methodology, Resources, Supervision, Investigation, Writing– review & editing. Yisong Li: Investigation, Methodology, Software. Junfei Yao: Writing– original draft, Conceptualization, Formal analysis, Data curation, Software. Jialu Wang: Methodology, Investigation, Software. Linlyu Han: Funding acquisition, Methodology. Qingqing Ma: Investigation, Software. Taimei Deng: Investigation, Validation. Ling Liao: Investigation, Validation. Lijun Deng: Methodology, Investigation. Guochao Sun: Resources. Mingfei Zhang: Methodology. Xun Wang: Funding acquisition, Methodology. Siya He: Software. Jiaxian He: Methodology. Zhihui Wang: Funding acquisition, Supervision, Writing– review & editing, Project administration.

Funding

The Department of Science and Technology in Sichuan Province, China, supported this research, grant number 2025YFHZ0081.

Data availability

The resulting RNA sequencing data was submitted to the NCBI's SRA under BioProject ID: PRJNA1061745.

Declarations

Ethics approval and consent to participate

Not applicable.

Consent to publish

Not applicable.

Competing interests

The authors declare no competing interests.

Author details

[1]College of Horticulture, Sichuan Agricultural University, Chengdu 611130, China

Received: 8 November 2024 / Accepted: 17 March 2025
Published online: 27 March 2025

References

1. Sahamishirazi S, Moehring J, Claupein W, Graeff-Hoenninger S. Quality assessment of 178 cultivars of Plum regarding phenolic, anthocyanin and sugar content. Food Chem. 2017;214:694–701. https://doi.org/10.1016/j.foodchem.2016.07.070.
2. Liu W, Nan G, Nisar MF, Wan C. Chemical constituents and health benefits of four Chinese Plum species. J Food Qual. 2020;2020:8842506. https://doi.org/10.1155/2020/8842506.
3. Jin W, Wang H, Li M, Wang J, Yang Y, Zhang X, Yan G, Zhang H, Liu J, Zhang K. The R2R3 MYB transcription factor PavMYB10.1 involves in anthocyanin

biosynthesis and determines fruit skin colour in sweet Cherry (*Prunus avium* L). Plant Biotechnol J. 2016;14(11):2120–33. https://doi.org/10.1111/pbi.12568.
4. Xu J, Xiong L, Yao J-L, Zhao P, Jiang S, Sun X, Dong C, Jiang H, Xu X, Zhang Y. Hypermethylation in the promoter regions of flavonoid pathway genes is associated with skin color fading during 'daihong' Apple fruit development. Hortic Res. 2024;11(3):uhae031. https://doi.org/10.1093/hr/uhae031.
5. Usenik V, Štampar F, Veberič R. Anthocyanins and fruit colour in plums (*Prunus domestica* L.) during ripening. Food Chem. 2009;114(2):529–34. https://doi.org/10.1016/j.foodchem.2008.09.083.
6. Jaakola L. New insights into the regulation of anthocyanin biosynthesis in fruits. Trends Plant Sci. 2013;18(9):477–83. https://doi.org/10.1016/j.tplants.2013.06.003.
7. Zhang M, Li Y, Wang J, Shang S, Wang H, Yang X, Lu C, Wang M, Sun X, Liu X, et al. Integrated transcriptomic and metabolomic analyses reveals anthocyanin biosynthesis in leaf coloration of Quinoa (*Chenopodium Quinoa* Willd). BMC Plant Biol. 2024;24(1):203. https://doi.org/10.1186/s12870-024-04821-2.
8. Xie Y, Tan H, Ma Z, Huang J. DELLA proteins promote anthocyanin biosynthesis via sequestering MYBL2 and JAZ suppressors of the MYB/bHLH/WD40 complex in *Arabidopsis Thaliana*. Mol Plant. 2016. https://doi.org/10.1016/j.molp.2016.01.014.
9. Feller A, Machemer K, Braun EL, Grotewold E. Evolutionary and comparative analysis of MYB and bHLH plant transcription factors. Plant J. 2011;66(1):94–116. https://doi.org/10.1111/j.1365-313X.2010.04459.x.
10. Ma Y, Ma X, Gao X, Wu W, Zhou B. Light induced regulation pathway of anthocyanin biosynthesis in plants. Int J Mol Sci. 2021. https://doi.org/10.3390/ijms222011116.
11. Fang Z, Lin-Wang K, Jiang C, Zhou D, Lin Y, Pan S, Espley RV, Ye X. Postharvest temperature and light treatments induce anthocyanin accumulation in Peel of 'akihime' Plum (*Prunus salicina* Lindl.) via transcription factor PsMYB10.1. Postharvest Biol Technol. 2021;179:111592. https://doi.org/10.1016/j.postharvbio.2021.111592.
12. Zhou H, Liao L, Xu S, Ren F, Zhao J, Ogutu C, Wang L, Jiang Q, Han Y. Two amino acid changes in the R3 repeat cause functional divergence of two clustered MYB10 genes in Peach. Plant Mol Biol. 2018;98(1):169–83. https://doi.org/10.1007/s11103-018-0773-2.
13. Fiol A, García-Gómez BE, Jurado-Ruiz F, Alexiou K, Howad W, Aranzana MJ. Characterization of Japanese Plum *(Prunus salicina*) PsMYB10 alleles reveals structural variation and polymorphisms correlating with fruit skin color. Front Plant Sci. 2021;12. https://doi.org/10.3389/fpls.2021.655267.
14. Chen M, Cao X, Huang Y, Zou W, Liang X, Yang Y, Wang Y, Wei J, Li H. The bZIP transcription factor MpbZIP9 regulates anthocyanin biosynthesis in *Malus* 'pinkspire' fruit. Plant Sci. 2024;342:112038. https://doi.org/10.1016/j.plantsci.2024.112038.
15. Xu R, Wang Y, Wang L, Zhao Z, Cao J, Fu D, Jiang W. PsERF1B-PsMYB10.1-PsbHLH3 module enhances anthocyanin biosynthesis in the flesh-reddening of amber-fleshed Plum (cv. Friar) fruit in response to cold storage. Hortic Res. 2023;10(6):uhad091. https://doi.org/10.1093/hr/uhad091.
16. Wang Y, An H, Yang Y, Yi C, Duan Y, Wang Q, Guo Y, Yao L, Chen M, Meng J, et al. The MpNAC72/MpERF105-MpMYB10b module regulates anthocyanin biosynthesis in *Malus* 'profusion' leaves infected with *Gymnosporangium Yamadae*. Plant J. 2024. n/a(n/a)https://doi.org/10.1111/tpj.16697.
17. Tao H, Gao F, Linying L, He Y, Zhang X, Wang M, Wei J, Zhao Y, Zhang C, Wang Q et al. WRKY33 negatively regulates anthocyanin biosynthesis and cooperates with PHR1 to mediate acclimation to phosphate starvation. Plant Commun 2024:100821. https://doi.org/10.1016/j.xplc.2024.100821
18. Gao H-N, Jiang H, Cui J-Y, You C-X, Li Y-Y. Review: the effects of hormones and environmental factors on anthocyanin biosynthesis in Apple. Plant Sci. 2021;312:111024. https://doi.org/10.1016/j.plantsci.2021.111024.
19. Nardozza S, Boldingh HL, Kashuba MP, Feil R, Jones D, Thrimawithana AH, Ireland HS, Philippe M, Wohlers MW, McGhie TK, et al. Carbon starvation reduces carbohydrate and anthocyanin accumulation in red-fleshed fruit via Trehalose 6-phosphate and MYB27. Plant Cell Environ. 2019. https://doi.org/10.1111/pce.13699.
20. Wang Y, Xiao Y, Sun Y, Zhang X, Du B, Turupu M, Yao Q, Gai S, Tong S, Huang J, et al. Two B-box proteins, PavBBX6/9, positively regulate light-induced anthocyanin accumulation in sweet Cherry. Plant Physiol. 2023;192(3):2030–48. https://doi.org/10.1093/plphys/kiad137.
21. Liu D, Zhao D, Li X, Zeng Y. AtGLK2, an Arabidopsis GOLDEN2-LIKE transcription factor, positively regulates anthocyanin biosynthesis via AtHY5-mediated light signaling. Plant Growth Regul. 2022;96(1):79–90. https://doi.org/10.1007/s10725-021-00759-9.
22. Zhang X, Yu L, Zhang M, Wu T, Song T, Yao Y, Zhang J, Tian J. MdWER interacts with MdERF109 and MdJAZ2 to mediate Methyl jasmonate- and light-induced anthocyanin biosynthesis in Apple fruit. Plant J. 2024;118(5):1327–42. https://doi.org/10.1111/tpj.16671.
23. Li H, Bai Y, Yang Y, Zheng H, Xu X, Li H, Wang W, Tao J. Transcriptomic analyses reveal light-regulated anthocyanin accumulation in 'ZhongShan-HongYu' grape berries. Sci Hort. 2023;309:111669. https://doi.org/10.1016/j.scienta.2022.111669.
24. Ni J, Liao Y, Zhang M, Pan C, Yang Q, Bai S, Teng Y. Blue light simultaneously induces Peel anthocyanin biosynthesis and flesh carotenoid/sucrose biosynthesis in Mango fruit. J Agric Food Chem. 2022;70(50):16021–35. https://doi.org/10.1021/acs.jafc.2c07137.
25. Jaakola L, Poole M, Jones MO, Kämäräinen-Karppinen T, Koskimäki JJ, Hohtola A, Häggman H, Fraser PD, Manning K, King GJ, et al. A SQUAMOSA MADS box gene involved in the regulation of anthocyanin accumulation in Bilberry fruits. Plant Physiol. 2010;153(4):1619–29. https://doi.org/10.1104/pp.110.158279.
26. Zhao L, Zhang Y, Sun J, Yang Q, Cai Y, Zhao C, Wang F, He H, Han Y. PpHY5 is involved in anthocyanin coloration in the Peach flesh surrounding the stone. Plant J. 2023;114(4):951–64. https://doi.org/10.1111/tpj.16189.
27. Wang Y, Zhang X, Zhao Y, Yang J, He Y, Li G, Ma W, Huang X, Su J. Transcription factor PyHY5 binds to the promoters of PyWD40 and PyMYB10 and regulates its expression in red Pear 'Yunhongli 1'. Plant Physiol Biochem. 2020;154:665–74. https://doi.org/10.1016/j.plaphy.2020.07.008.
28. Zhang N, Wei C-Q, Xu D-J, Deng Z-P, Zhao Y-C, Ai L-F, Sun Y, Wang Z-Y, Zhang S-W. Photoregulatory protein kinases fine-tune plant photomorphogenesis by directing a bifunctional phospho-code on HY5 in Arabidopsis. Dev Cell. 2024. https://doi.org/10.1016/j.devcel.2024.04.007.
29. Liang D, Zhu T, Deng Q, Lin L, Tang Y, Wang J, Wang X, Luo X, Zhang H, Lv X, et al. PacCOP1 negatively regulates anthocyanin biosynthesis in sweet Cherry (*Prunus avium* L). J Photochem Photobiol B. 2020;203:111779. https://doi.org/10.1016/j.jphotobiol.2020.111779.
30. Liu Y, Zhang X-W, Liu X, Zheng P-F, Su L, Wang G-L, Wang X-F, Li Y-Y, You C-X, An J-P. Phytochrome interacting factor MdPIF7 modulates anthocyanin biosynthesis and hypocotyl growth in Apple. Plant Physiol. 2022;188(4):2342–63. https://doi.org/10.1093/plphys/kiab605.
31. Qin J, Zhao C, Wang S, Gao N, Wang X, Na X, Wang X, Bi Y. PIF4-PAP1 interaction affects MYB-bHLH-WD40 complex formation and anthocyanin accumulation in *Arabidopsis*. J Plant Physiol. 2022;268:153558. https://doi.org/10.1016/j.jplph.2021.153558.
32. Deng L, Wang T, Hu J, Yang X, Yao Y, Jin Z, Huang Z, Sun G, Xiong B, Liao L, et al. Effects of pollen sources on fruit set and fruit characteristics of 'fengtangli' Plum (*Prunus salicina* Lindl.) based on microscopic and transcriptomic analysis. Int J Mol Sci. 2022. https://doi.org/10.3390/ijms232112959.
33. Yao L, Liang D, Xia H, Pang Y, Xiao Q, Huang Y, Zhang W, Pu C, Wang J, Lv X. Biostimulants promote the accumulation of carbohydrates and biosynthesis of anthocyanins in 'yinhongli' Plum. Front Plant Sci. 2023;13. https://doi.org/10.3389/fpls.2022.1074965.
34. Huan C, Xu Q, Shuling S, Dong J, Zheng X. Effect of benzothiadiazole treatment on quality and anthocyanin biosynthesis in Plum fruit during storage at ambient temperature. J Sci Food Agric. 2021;101(8):3176–85. https://doi.org/10.1002/jsfa.10946.
35. Liu Y, Feng X, Zhang Y, Zhou F, Zhu P. Simultaneous changes in anthocyanin, chlorophyll, and carotenoid contents produce green variegation in pink–leaved ornamental Kale. BMC Genomics. 2021;22(1):455. https://doi.org/10.1186/s12864-021-07785-x.
36. Zhishen J, Mengcheng T, Jianming W. The determination of flavonoid contents in mulberry and their scavenging effects on superoxide radicals. Food Chem. 1999;64(4):555–9. https://doi.org/10.1016/S0308-8146(98)00102-2.
37. Xiong B, Li Q, Yao J, Zheng W, Ou Y, He Y, Liao L, Wang X, Deng H, Zhang M, et al. Transcriptome and UPLC-MS/MS reveal mechanisms of amino acid biosynthesis in sweet orange 'newhall' after different rootstocks grafting. Front Plant Sci. 2023. https://doi.org/10.3389/fpls.2023.1216826.
38. Li Q, Yao J, Zheng W, Wang J, Liao L, Sun G, Wang X, Deng H, Zhang M, Wang Z, et al. Hetero-grafting affects flavonoid biosynthesis in sweet orange 'Newhall' (*Citrus sinensis*) peels: a metabolomics and transcriptomics analysis. Front Plant Sci. 2023;14. https://doi.org/10.3389/fpls.2023.1218426.
39. Zhang J, Feng R, Xing X, Hou W, Mu X, Zhang J, Gao YG, Du J, Wang P. Transcriptome and weighted gene co-expression network analysis reveal key genes involved in the Proanthocyanidin biosynthesis in *Cerasus humilis*. Sci Hort. 2024;325:112717. https://doi.org/10.1016/j.scienta.2023.112717.

40. Peng T, Saito T, Honda C, Ban Y, Kondo S, Liu J-H, Hatsuyama Y, Moriguchi T. Screening of UV-B-induced genes from Apple peels by SSH: possible involvement of MdCOP1-mediated signaling cascade genes in anthocyanin accumulation. Physiol Plant. 2012. https://doi.org/10.1111/ppl.12002.
41. Ma C, Liang B, Chang B, Yan J, Liu L, Wang Y, Yang Y, Zhao Z. Transcriptome profiling of anthocyanin biosynthesis in the Peel of 'granny Smith' apples (*Malus domestica*) after bag removal. BMC Genomics. 2019;20(1):353. https://doi.org/10.1186/s12864-019-5730-1.
42. Ferreyra MLF, Serra P, Casati P. Recent advances on the roles of flavonoids as plant protective molecules after UV and high light exposure. Physiol Plant. 2021;173(3):736–49. https://doi.org/10.1111/ppl.13543.
43. Nam TG, Kim D-O, Eom SH. Effects of light sources on major flavonoids and antioxidant activity in common buckwheat sprouts. Food Sci Biotechnol. 2018;27(1):169–76. https://doi.org/10.1007/s10068-017-0204-1.
44. Henry-Kirk RA, Plunkett B, Hall M, McGhie T, Allan AC, Wargent JJ, Espley RV. Solar UV light regulates flavonoid metabolism in Apple (Malus X *domestica*). Plant Cell Environ. 2018;41(3):675–88. https://doi.org/10.1111/pce.13125.
45. Fu B, Ji X, Zhao M, He F, Wang X, Wang Y, Liu P, Niu L. The influence of light quality on the accumulation of flavonoids in tobacco (*Nicotiana tabacum* L.) leaves. J Photochem Photobiol B. 2016;162:544–9. https://doi.org/10.1016/j.jphotobiol.2016.07.016.
46. Li C, Wan Y, Shang X, Fang S. Integration of transcriptomic and metabolomic analysis unveils the response mechanism of sugar metabolism in *Cyclocarya Paliurus* seedlings subjected to PEG-induced drought stress. Plant Physiol Biochem. 2023;201:107856. https://doi.org/10.1016/j.plaphy.2023.107856.
47. Huang H, Abid M, Lin M, Wang R, Gu H, Li Y, Qi X. Comparative transcriptome analysis of different *Actinidia Arguta* fruit parts reveals difference of light response during fruit coloration. Biology. 2021. https://doi.org/10.3390/biology10070648.
48. Jeong S-W, Das PK, Jeoung SC, Song J-Y, Lee HK, Kim Y-K, Kim WJ, Park YI, Yoo S-D, Choi S-B, et al. Ethylene suppression of sugar-induced anthocyanin pigmentation in *Arabidopsis*. Plant Physiol. 2010;154(3):1514–31. https://doi.org/10.1104/pp.110.161869.
49. Schmitz J, Heinrichs L, Scossa F, Fernie AR, Oelze M-L, Dietz K-J, Rothbart M, Grimm B, Flügge U-I, Häusler RE. The essential role of sugar metabolism in the acclimation response of *Arabidopsis Thaliana* to high light intensities. J Exp Bot. 2014;65(6):1619–36. https://doi.org/10.1093/jxb/eru027.
50. Zirngibl M-E, Araguirang GE, Kitashova A, Jahnke K, Rolka T, Kühn C, Nägele T, Richter AS. Triose phosphate export from chloroplasts and cellular sugar content regulate anthocyanin biosynthesis during high light acclimation. Plant Commun. 2023;4(1):100423. https://doi.org/10.1016/j.xplc.2022.100423.
51. Do VG, Lee Y, Kim J-H, Kwon Y-S, Park J-T, Yang S, Park J, Win NM, Kim S. The synergistic effects of environmental and genetic factors on the regulation of anthocyanin accumulation in plant tissues. Int J Mol Sci. 2023. https://doi.org/10.3390/ijms241612946.
52. Stracke R, Ishihara H, Huep G, Barsch A, Mehrtens F, Niehaus K, Weisshaar B. Differential regulation of closely related R2R3-MYB transcription factors controls flavonol accumulation in different parts of the *Arabidopsis Thaliana* seedling. Plant J. 2007;50(4):660–77. https://doi.org/10.1111/j.1365-313X.2007.03078.x.
53. Fornalé S, Lopez E, Salazar-Henao JE, Fernández-Nohales P, Rigau J, Caparros-Ruiz D. AtMYB7, a new player in the regulation of UV-sunscreens in *Arabidopsis Thaliana*. Plant Cell Physiol. 2014;55(3):507–16. https://doi.org/10.1093/pcp/pct187.
54. Gonzalez A, Zhao M, Leavitt JM, Lloyd AM. Regulation of the anthocyanin biosynthetic pathway by the TTG1/bHLH/Myb transcriptional complex in Arabidopsis seedlings. Plant J. 2008;53(5):814–27. https://doi.org/10.1111/j.1365-313X.2007.03373.x.
55. Shin DH, Choi M, Kim K, Bang G, Cho M, Choi S-B, Choi G, Park Y-I. HY5 regulates anthocyanin biosynthesis by inducing the transcriptional activation of the MYB75/PAP1 transcription factor in *Arabidopsis*. FEBS Lett. 2013;587(10):1543–7. https://doi.org/10.1016/j.febslet.2013.03.037.
56. Yang T, Ma H, Li Y, Zhang Y, Zhang J, Wu T, Song T, Yao Y, Tian J. Apple MPK4 mediates phosphorylation of MYB1 to enhance light-induced anthocyanin accumulation. Plant J. 2021;106(6):1728–45. https://doi.org/10.1111/tpj.15267.
57. Aharoni A, De Vos CHR, Wein M, Sun Z, Greco R, Kroon A, Mol JNM, O'Connell AP. The strawberry FaMYB1 transcription factor suppresses anthocyanin and flavonol accumulation in Transgenic tobacco. Plant J. 2001;28(3):319–32. https://doi.org/10.1046/j.1365-313X.2001.01154.x.
58. Zhou K, Wang J, Pan L, Xiang F, Zhou Y, Xiong W, Zeng M, Grierson D, Kong W, Hu L, et al. A chromosome-level genome assembly for Chinese Plum 'wushancuili' reveals the molecular basis of its fruit color and susceptibility to rain-cracking. Hortic Plant J. 2023. https://doi.org/10.1016/j.hpj.2023.04.011.
59. Fiol A, García S, Dujak C, Pacheco I, Infante R, Aranzana MJ. An LTR retrotransposon in the promoter of a PsMYB10.2 gene associated with the regulation of fruit flesh color in Japanese Plum. Hortic Res. 2022;9:uhac206. https://doi.org/10.1093/hr/uhac206.
60. Lotkowska ME, Tohge T, Fernie AR, Xue G-P, Balazadeh S, Mueller-Roeber B. The *Arabidopsis* transcription factor MYB112 promotes anthocyanin formation during salinity and under high light stress. Plant Physiol. 2015;169(3):1862–80. https://doi.org/10.1104/pp.15.00605.
61. Guo X, Wang Y, Zhai Z, Huang T, Zhao D, Peng X, Feng C, Xiao Y, Li T. Transcriptomic analysis of light-dependent anthocyanin accumulation in bicolored Cherry fruits. Plant Physiol Biochem. 2018;130:663–77. https://doi.org/10.1016/j.plaphy.2018.08.016.
62. An J-P, Qu F-J, Yao J-F, Wang X-N, You C-X, Wang X-F, Hao Y-J. The bZIP transcription factor MdHY5 regulates anthocyanin accumulation and nitrate assimilation in Apple. Hortic Res. 2017;4. https://doi.org/10.1038/hortres.2017.23.
63. Sun Q, Jiang S, Zhang T, Xu H, Fang H, Zhang J, Su M, Wang Y, Zhang Z, Wang N, et al. Apple NAC transcription factor MdNAC52 regulates biosynthesis of anthocyanin and Proanthocyanidin through MdMYB9 and MdMYB11. Plant Sci. 2019;289:110286. https://doi.org/10.1016/j.plantsci.2019.110286.
64. Shin J, Park E, Choi G. PIF3 regulates anthocyanin biosynthesis in an HY5-dependent manner with both factors directly binding anthocyanin biosynthetic gene promoters in *Arabidopsis*. Plant J. 2007;49(6):981–94. https://doi.org/10.1111/j.1365-313X.2006.03021.x.
65. Paik I, Huq E. Plant photoreceptors: Multi-functional sensory proteins and their signaling networks. Semin Cell Dev Biol. 2019;92:114–21. https://doi.org/10.1016/j.semcdb.2019.03.007.
66. Jiang M, Ren L, Lian H, Liu Y, Chen H. Novel insight into the mechanism underlying light-controlled anthocyanin accumulation in eggplant (*Solanum melongena* L). Plant Sci. 2016;249:46–58. https://doi.org/10.1016/j.plantsci.2016.04.001.

Publisher's note